J Paleolimnol (2010) 44:413–429
DOI 10.1007/s10933-010-9412-x

ORIGINAL PAPER

ENSO and solar activity signals from oxygen isotopes in diatom silica during late glacial-Holocene transition in Central Andes (18°S)

Armand Hernández · Santiago Giralt · Roberto Bao · Alberto Sáez · Melanie J. Leng · Philip A. Barker

Received: 8 April 2009 / Accepted: 1 February 2010 / Published online: 21 February 2010

Abstract The late glacial-Holocene transition from the Lago Chungará sedimentary record in northern Chilean Altiplano (18°S) is made up of laminated sediments composed of light-white and dark-green pluriannual couplets of diatomaceous ooze. Light-white sediment laminae accumulated during short-term extraordinary diatom blooms whereas dark-green sediment laminae represent the baseline limnological conditions during several years of deposition. Diatom oxygen isotope ratios ($\delta^{18}O_{diatom}$) from 40 consecutive dark-green laminae, ranging from 11,990 to 11,450 cal year BP, show that a series of decadal-to-centennial dry–wet oscillations occurred. Dry periods are marked by relatively high isotope values whereas wet episodes are indicated by lower values. This interpretation agrees with the reconstructions of terrigenous inputs and regional effective moisture availability carried out in the lake but there is a systematic temporal disagreement between them owing to the non-linear response of the lacustrine ecosystem to environmental forcings. Furthermore, the $\delta^{18}O_{diatom}$ record tracks effective moisture changes at a centennial scale. Three major phases have been established (11,990–11,800, 11,800–11,550, and 11,550–11,450 cal year BP). Each phase is defined by an increasing isotope trend followed by a sudden depletion. In addition, several wet and dry events at a decadal scale are superimposed onto these major trends. Spectral analyses of the $\delta^{18}O_{diatom}$ values suggest that cycles and events could have been triggered by both El Niño-Southern Oscillation (ENSO) and solar activity. Significant ENSO frequencies of 7–9 years and 15–17 years, and periodicities of the solar activity cycles such as 11 years (Schwabe), 23 years (Hale) and 35 years (Brückner) have been recognised in the oxygen isotope time series. Time–frequency analysis shows that although solar and ENSO forcing were present at the onset of the Holocene, they were more intense during the late glacial period. The early Holocene might have been mainly governed by La Niña-like

A. Hernández (✉) · S. Giralt
Institute of Earth Sciences Jaume Almera-CSIC, C/Lluís Solé i Sabarís s/n, 08028 Barcelona, Spain
e-mail: ahernandez@ija.csic.es

R. Bao
Faculty of Sciences, University of A Coruña, Campus da Zapateira s/n, 15701 A Coruña, Spain

A. Sáez
Faculty of Geology, University of Barcelona, C/Martí Franquès s/n, 08028 Barcelona, Spain

M. J. Leng
NERC Isotope Geosciences Laboratory, British Geological Survey, Nottingham NG12 5GG, UK

M. J. Leng
School of Geography, University of Nottingham, Nottingham NG7 2RD, UK

P. A. Barker
Lancaster Environment Centre, Lancaster University, Lancaster LA1 4YQ, UK

conditions that correspond to wet conditions over the Andean Altiplano.

Keywords Lake · Oxygen isotopes · Late glacial · Holocene · Andean altiplano · ENSO · Solar activity · Diatoms

Introduction

The study of Andean Altiplano lacustrine records plays a prominent role for interpreting the Quaternary palaeoclimatic history of the South American tropics and therefore for understanding the function of the tropics in the Earth's climate system (Grosjean et al. 2001; Valero-Garcés et al. 2003; Placzek et al. 2006) (Fig. 1). For this reason, studies on the sedimentary records from this area have increased in the last few decades. Most of these studies have focussed on the reconstruction of climatic events at millennial time scales, especially since the Last Glacial Maximum (Baker et al. 2001a). There is a general consensus that orbital forces are the main factor triggering the climatic conditions at a millennial-scale (Rowe et al. 2002; Placzek et al. 2006), and are therefore responsible for those climatic events. Superimposed onto

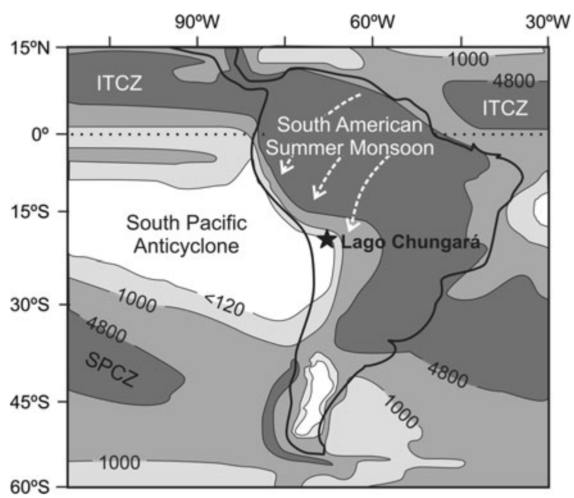

Fig. 1 Location of Lago Chungará on a South America rainfall rate map (mm/year) simplified from Negri et al. (2004). Main atmospheric systems are indicated. ICTZ: Intertropical Convergence Zone, SPCZ: South Pacific Convergence Zone

this long term variability, changes in the hydrologic balance at a sub-millennial scale in the Andean Altiplano, have been attributed to the variability of the Pacific Sea Surface Temperatures (SSTs) and the strength of the zonal winds (Rowe et al. 2002; Garreaud et al. 2003). Both factors are controlled by El Niño-Southern Oscillation (ENSO) and changes in the solar activity (Theissen et al. 2008). A number of studies have detected multidecadal- to centennial-scale hydrological balance shifts, suggesting that these relationships have been active since, at least, the mid-Holocene (Valero-Garcés et al. 2003; Theissen et al. 2008).

Diatom oxygen isotopes ($\delta^{18}O_{diatom}$) are increasingly being used for palaeoenvironmental reconstructions in lacustrine sedimentary records (Rietti-Shati et al. 1998; Barker et al. 2001). However, application of this proxy to high-resolution centennial to millennial lacustrine records is still in its infancy (Barker et al. 2007). $\delta^{18}O_{diatom}$ in decadal-to-centennial resolution palaeoclimatic reconstructions has not been utilised, mainly due to the difficulty in obtaining high resolution samples from sites with sufficient variation in $\delta^{18}O_{diatom}$ (outside of analytical error) that can be characterised at this fine temporal scale. Additional difficulties in using $\delta^{18}O_{diatom}$ are related to the difficulty in obtaining monospecific diatom samples in order to eliminate any species-specific effect variability, to acquire the necessary amount of sample from these short periods of time, and to have pure diatom samples, since significant contaminants can produce excursions in $\delta^{18}O_{diatom}$ that are similar to those produced by climate variations (Brewer et al. 2008).

The diatomaceous ooze from Lago Chungará has previously been the subject of a preliminary diatom oxygen isotope study at low resolution. This earlier study was aimed at three non-consecutive stretches of the sedimentary record, and did not include all the dark-green laminae (Hernández et al. 2008). For the present study we have analysed 40 consecutive dark-green laminae, corresponding to the late glacial and early Holocene, which represent a continuous record of the background limnological conditions (Hernández et al. 2008) (see the sedimentary model in the sedimentary sequence and rhythmite type section below). The excellent preservation and high diatom content of the record of Lago Chungará allow a detailed study of the regional moisture balance at decadal and centennial timescales.

Here, we present the decadal-to-centennial time scale moisture balance reconstruction for the Andean Altiplano during the late glacial-Holocene transition (11,990–11,450 cal year BP) based on high-resolution analysis of $\delta^{18}O_{diatom}$. This analysis was performed on successive and continuous 40 dark-green laminae of lacustrine sediments present in a core located in the offshore zone of Lago Chungará. In order to support the interpretation, isotope data are compared with the reconstructions of the terrigenous inputs and inferred regional effective moisture in the Lago Chungará performed in the same core by Giralt et al. (2008).

Lago Chungará setting

Geology and hydrology

Lago Chungará (18°15′S, 69°10′W, 4,520 m a.s.l.) is located in the Chilean Altiplano (Central Andes) lying in a highly active tectonic and volcanic context (Hora et al. 2007). The lake sits in the small hydrologically closed Chungará sub-Basin which was formed as a result of a debris avalanche during the partial collapse of the Parinacota Volcano, damming the former Lauca River (Fig. 2). Lago Chungará and Lagunas Cotacotani were formed almost immediately. However, the age of this collapse is not well constrained, with estimates ranging from 13,000 to 20,000 year BP (Hora et al. 2007).

The lake has an irregular shape with a maximum length of 8.75 km, maximum water depth of 40 m, a surface area of 21.5 km^2 and a volume of 400×10^6 m^3 (Mühlhauser et al. 1995; Herrera et al. 2006) (Fig. 2a). At present, the main inlet to the lake is the Chungará River (300–460 l s^{-1}) although secondary streams enter to the lake in the south-western margin. Evaporation is the main water loss (3×10^7 m^3 $year^{-1}$), and groundwater outflow from Lago Chungará to Lagunas Cotacotani (6–7 $\times 10^6$ m^3 $year^{-1}$, Dorador et al. 2003) represents about 20% of the total outflow. The calculated residence time for the lakewater is approximately 15 years (Herrera et al. 2006). Water inputs to the lake have, on average, the following composition: 42 ppm HCO_3^-, 3 ppm Cl^-, 17 ppm SO_4^{2-}, 7 ppm Na^+, 4 ppm Mg^{2+}, 8 ppm Ca^{2+}, 3 ppm K^+ and 22 ppm Si. The Mg/Ca ratio of water inputs ranges from 0.22 to 0.71, depending on the local lithology of the catchment (Herrera et al. 2006; Sáez et al. 2007). Isotope data, temperature, pH, O_2 and conductivity profiles of the lake water and the water inputs to the lake are shown in Table 1. The lake can be considered as polymictic and oligo- to meso-eutrophic (Mühlhauser et al. 1995). The $\delta^{18}O$ and δD composition of the lake water reveal that it diverges from the Global Meteoric Water Line

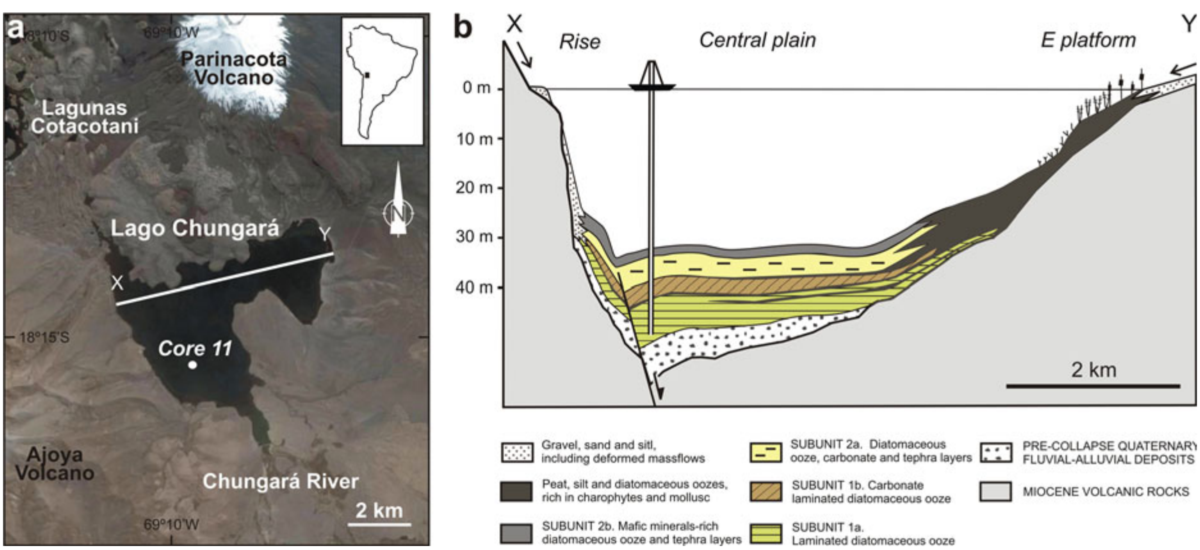

Fig. 2 **a** Location of the Chungará-Cotacotani lake district (modified from Google Earth). **b** Cross section of sediments infilling Lago Chungará. Position of core 11 is shown; note that the position of the core is projected in its equivalent position at the lake central plain. *Arrows* indicate major hydrological inputs and sedimentary contributions to the lake. Simplified from Sáez et al. (2007)

Table 1 Isotopic and other chemical and physical data analysed from water samples collected in the Lago Chungará (Modified from Herrera et al. 2006)

Site	Depth (m)	Date	$\delta^{18}O$	δD	$\delta^{13}C$	Conductivity ($\mu S\ cm^{-1}$)	pH	Temp (°C)	O_2
Lake									
Chungará	0	Nov-02	−1.52	−42.0	4.96	1,444	9.30	9.1	12.10
Chungará	20	Nov-02	−1.62	−42.6	4.26	1,433	9.17	7.2	7.80
Chungará	0	Jan-02	−3.85	−48.8	NA	1,262	9.63	17	NA
Chungará	2	Nov-02	−1.54	−44	NA	1,423	9.23	10.2	9.10
Chungará	2	Nov-02	−1.58	−44.7	4.62	1,451	9.23	9.9	9.30
Chungará	5	Nov-02	−1.53	−43.2	5.52	1,462	9.17	9.5	8.90
Chungará	20	Nov-02	−1.59	−44.4	5.34	1,455	9.05	7.1	7.60
Chungará	0	Nov-02	−1.49	−44,2	5.43	1,473	9.20	12.1	11.90
Chungará	5	Nov-02	NA	NA	NA	1,461	NA	9.5	NA
Chungará	10	Nov-02	NA	NA	NA	1,459	NA	9	NA
Chungará	15	Nov-02	NA	NA	NA	1,458	NA	8.1	NA
Chungará	20	Nov-02	NA	NA	NA	1,457	NA	7.6	NA
Chungará	25	Nov-02	NA	NA	NA	1,457	NA	7	NA
Chungará	31	Nov-02	−1.61	−45.8	−3.55	NA	9.02	NA	NA
Chungará	2	Nov-02	−1.50	−44.3	5.97	1,464	9.20	9.9	NA
Chungará	21	Nov-02	−1.76	−41.7	3.68	1,473	9.08	7.6	NA
Chungará	0	Nov-02	NA	NA	NA	1,464	NA	10.4	NA
Chungará	5	Nov-02	NA	NA	NA	1,461	NA	9.6	NA
Chungará	10	Nov-02	NA	NA	NA	1,461	NA	9.3	NA
Chungará	15	Nov-02	NA	NA	NA	1,461	NA	9.1	NA
Chungará	20	Nov-02	NA	NA	NA	1,456	9.15	7.2	NA
Chungará	25	Nov-02	NA	NA	NA	1,456	NA	7	NA
Chungará	30	Nov-02	NA	NA	NA	1,455	NA	6.8	NA
Chungará	35	Nov-02	NA	NA	NA	1,454	NA	6.4	NA
Chungará	0	Nov-02	−1.56	−39.9	3.21	1,439	9.08	9	11.20
Chungará	15	Nov-02	−1.54	−43.4	5.17	1,438	8.99	8.3	8.30
Chungará	33	Nov-02	−1.58	−43.4	4.56	1,435	9.10	6.2	6.20
Chungará	0	Nov-02	−2.05	−44.4	7.03	1,388	9.22	10.7	NA
Chungará	0	Jan-02	−3.39	−46.8	6.40	1,400	9.19	11.4	NA
Chungará	0	Jun-06	NA	NA	NA	1,463	9.42	5	10.50
Chungará	12	Jan-02	NA	NA	8.10	NA	NA	NA	NA
Chungará	0	Jun-06	NA	NA	NA	1,493	9.70	2	9.30
Chungará	0	Jun-06	NA	NA	NA	1,418	9.48	9	13.00
Chungará	0	Jun-06	NA	NA	NA	220	9.70	5	25.00
Springs									
Bofedal	0	Jan-02	−14.98	−116	−2.20	52	7.15	7.9	NA
Bofedal	0	Nov-02	−16.49	−116.6	−7.04	48.7	7.07	7.8	NA
Mal paso	0	Jan-02	−15.58	−120.5	NA	46.8	7.31	9.7	NA
Mal paso	0	Nov-02	−17.04	−121.9	−8.97	51.2	6.97	10/11.6	NA
Mal paso	0	Jan-04	−17.3	−121.3	NA	122	7.71	10.8	NA
Ajata	0	Jan-02	−14.07	−106.2	NA	59.8	7.80	7.6	NA

Table 1 continued

Site	Depth (m)	Date	δ^{18}O	δD	δ^{13}C	Conductivity (µS cm^{-1})	pH	Temp (°C)	O_2
Ajata	0	Nov-02	−15.28	−205.9	−6.86	50	7.46	5.3	NA
Canal	0	Nov-02	−17.12	−121.7	−10.14	66.7	8.09	10	NA
Canal	0	Jan-04	−17.26	−119.3	NA	380	7.62	9.4	NA
Colada Ajata	0	Jan-02	−14.88	−111	−2.80	155.1	5.82	4.9	NA
Colada Ajata	0	Nov-02	−16.23	−112.1	−2.69	136.1	5.94	4.5	NA
River									
Chungará	0	Jan-02	−14.82	−111.8	NA	241	9.28	16	NA
Chungará	0	Nov-02	−16.09	−113.1	−1.15	223	8.99	17	NA
Chungará	0	Jan-04	−16.27	−114.1	NA	316	8.02	14.2	NA

NA not available data

(GMWL) and the Regional Meteoric Line (RML). This divergence can be attributed to the enrichment of the lake water by evaporation with regard to rainfall and springwater (Fig. 3a; Herrera et al. 2006). The mean lake water values of δ^{18}O and δD (January 2002 to January 2004) are −1.4‰ SMOW and −43.4‰ SMOW, respectively (Table 1).

Climate

Climate in the Chungará-Cotacotani lake district is dominated by arid conditions due to the influence of the South Pacific Anticyclone (Fig. 1). Modern mean annual temperature at Lago Chungará is +4.2°C. Annual rainfall ranges from 100 to 750 mm year^{-1} (mean 411 mm year^{-1}), losing 1,200 mm year^{-1} via evaporation, which exceeds precipitation (Fig. 3b; Valero-Garcés et al. 2000). The lake region shows pronounced seasonal contrasts due to the dominance of the tropical summer moisture (Garreaud et al. 2003), known as the South American Summer Monsoon (SASM) (Vuille and Werner 2005). Regional moisture originates from the tropical Atlantic Ocean and is transported to the Altiplano throughout Amazonia during the summer months (DJFM). During these months weak easterly flow prevails over the Altiplano as a consequence of the southward migration of the subtropical jet stream and the establishment of the Bolivian high-pressure system (Garreaud et al. 2003). This climatic situation defines this time window as the wet season in the Altiplano accounting for more than 70% of the annual precipitation (Fig. 3b). The SASM is a major component of the climate system over tropical and subtropical South America during the austral summer and is remotely forced by tropical Pacific SSTs (Vuille and Werner 2005). Thus, the inter-annual to decadal climate variability is currently related to ENSO-like variations over the Pacific basin (Valero-Garcés et al. 2003). Instrumental data from the Chungará area show a reduction of the precipitation during moderate to intense El Niño years (Fig. 3c). However, there is no direct relationship between the relative El Niño strength and the amount of rainfall reduction (Valero-Garcés et al. 2003). Furthermore, on longer timescales, it is speculated that changes in tropical-Atlantic meridional SST gradients also force precipitation variability on the Altiplano (Baker et al. 2001b).

Rainfall isotope composition in Central Andes (Fig. 3d) is characterised by a large variability in δ^{18}O (between +1.2 and −21.1‰) and of δD (between +22.5 and −160.1‰). The origin of the lightest oxygen isotope values is the strong fractionation in the air masses from the Amazon and is directly related to higher rainfall intensity (‘amount effect’) (Herrera et al. 2006). However, the rainfall oxygen isotope composition in the Chungará-Cotacotani lake district only oscillates by 6‰, between −14 and −20‰, with a mean value of −14.3‰ (Fig. 3a, d).

Sedimentary sequence and rhythmite type

The sedimentary infill of Lago Chungará was characterised by the lithological description of fifteen lake cores obtained in 2002 (Sáez et al. 2007) and by seismic imagery obtained in 1993 (Valero-Garcés et al. 2000; Sáez et al. 2007). From the bottom to the top of core 11,

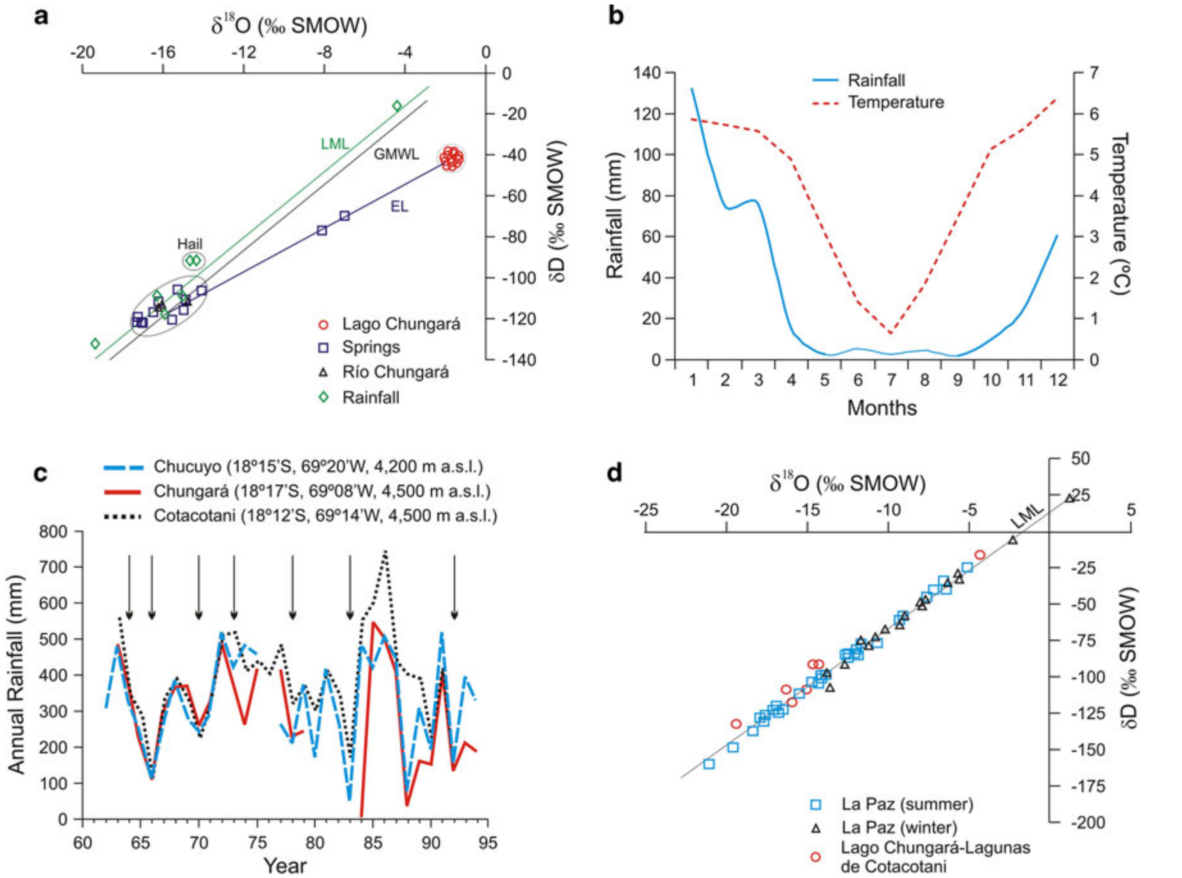

Fig. 3 **a** Isotope values ($\delta^{18}O/\delta D$) from rainfall, Lago Chungará, Río Chungará and studied area springs. GMWL: Global Meteoric Water Line; LML: Local Meteoric Line; EL: Evaporation Line. Note the isotopic enrichment of the lake water by evaporation with regard to rainfall and springwater. **b** Mean monthly rainfall (mm) and temperature (°C) at Chungará meteorological station (18.17S, 69.08W, 4,500 m a.s.l.). Note the seasonality of both parameters. **c** Annual rainfall in the Chungará region from 1962 to 1994. The arrows indicate strong El Niño years. Modified from Valero-Garcés et al. (2003). **d** Isotope composition ($\delta^{18}O/\delta D$) of rainfall samples from La Paz (Bolivia) obtained by the International Atomic Energy Agency (IAEA) since 1995 until 1998 (*blue squares* and *black triangles*), and the samples of Lago Chungará and the very close Lagunas de Cotacotani obtained from Herrera et al. (2006) (*red circles*). LML: Local Meteoric Line ($\delta D = 7.9\delta^{18}O + 14$). Note the variability in $\delta^{18}O$ and of δD values

two sedimentary units (units 1 and 2) were identified and correlated over the offshore zone of the lake mainly using tephra keybeds (Figs. 2a, 2b). Unit 1 is made up of diatomaceous ooze with variable types and quantities of carbonates (calcite, aragonite) and amorphous organic matter. It is continuous across the lake, although thickest in the NW sector of the central plain and thins towards the south and west, probably overlapping the Miocene substrate. Unit 1 occurs in the central plain and the sharply rising flank of the lake (Fig. 2b) and is divided in two subunits. Subunit 1a is composed by light-white and dark-green diatomaceous ooze couplets and a rhythmite type was defined (Hernández et al. 2008). Light-white laminae are formed by the skeletons of the diatom *Cyclostephanos andinus* (Theriot, Carney, and Richerson) Tapia, Theriot, Fritz, Cruces and Riv. Dark-green laminae, with higher organic matter content, are made up by a mixture of diatoms, including the euplanktonic *Cyclostephanos andinus*, although diatoms of the *Cyclotella stelligera* complex are co-dominant taxa. Subdominant groups are some tychoplanktonic (*Fragilaria* spp.) and benthic taxa (*Cocconeis* spp., *Achnanthes* spp., *Navicula* spp., *Nitzschia* spp.). Subunit 1b is composed of centimetre- to decimetre-thick laminated brown diatomaceous ooze and endogenic carbonates that occur in low concentrations. Unit 2 is about 6 m-thick and grades laterally to the west and south into alluvial and deltaic deposits, and towards the east into macrophyte, organic-rich facies (Fig. 2b). It is mainly composed of massive to slightly banded diatomaceous ooze interbedding with 13 tephra layers. Unit 2 is also divided in two subunits. Subunit 2a is composed of brownish-red massive to slightly banded sapropelic diatomaceous ooze with common calcitic crystals (silt grain-sized) and carbonate-rich layers. Subunit 2b consists of dark-grey diatomaceous ooze with frequent macrophyte remains alternating with massive black tephra layers, mainly composed of plagioclase, glass and mafic minerals (Sáez et al. 2007; Moreno et al. 2007).

The chronological model for the sedimentary sequence of Lago Chungará is based on 17 ^{14}C AMS dates obtained from bulk organic matter from the central plain cores and aquatic organic macrofossils picked from littoral cores, and one $^{238}U/^{230}Th$ date from carbonate. Details on the construction of the chronological framework are discussed elsewhere (Giralt et al. 2008). According to the chronological model, the studied interval records the late glacial-Holocene transition (11,990–11,450 cal year BP) and each couplet was deposited during time intervals ranging from 4 to 24 years. Light-white sediment laminae accumulated during short term diatom blooms (occurring from days to weeks) whereas dark-green sediment laminae represent the baseline limnological conditions during several years of deposition (Hernández et al. 2008).

Previous work has characterised the surface and underground waters from the Chungará and Cotacotani lake district (Herrera et al. 2006), as well as the sediments of Lago Chungará. X-Ray Fluorescence (XRF), X-Ray Diffraction (XRD), Total Carbon and Total Organic Carbon (TC and TOC), Total Biogenic Silica (TBSi), pollen and diatom analyses were performed. These multiproxy studies have allowed us to establish the sedimentary, hydrological and environmental evolution of the Lago Chungará at different time scales (Sáez et al. 2007; Moreno et al. 2007; Giralt et al. 2008).

Methods

An interval of 46.5 cm from the laminated dark-green and light-white sediments of Subunit 1a (deposited between 11,990 and 11,450 cal year BP) was selected and sampled, lamina by lamina, from core 11 (Fig. 2). All the dark-green laminae (40 samples) of this interval were selected for $\delta^{18}O_{diatom}$ analyses to carry out a very high-resolution study of the baseline environmental evolution of Lago Chungará (sampling ranging from 4.1 to 24.4 years; average temporal resolution is ca. 12 years) during the late glacial and early Holocene transition period. Of these, 22 samples were also previously used in a lower resolution study (Hernández et al. 2008). The thickness of the dark-green laminae sampled ranges between 2 and 9 mm.

Analysis of the oxygen isotope composition of diatom silica requires the material to be almost pure diatomite (Juillet-Leclerc 1986). Our samples were treated following the method proposed by Morley et al. (2004) with some variations (Hernández et al. 2008). The samples were treated to remove organics and carbonate, then sieved at 125 μm to eliminate resistant charcoal and terrigenous particles. The 63- and 38-μm sieves were used to obtain a diatom concentrate made up almost exclusively by large valves of the centric diatom *Cyclostephanos andinus,* eliminating in the samples any species-specific effect variability (Fig. 4). Gravity settling in a water column during the sieving process also helped to remove any remaining tephra and clay particles. The Gravitational Split-flow Thin Fractionation (SPLITT) was then applied to the most problematic samples, at Lancaster University (UK), as an alternative approach to heavy liquid separation (Rings et al. 2004; Leng and Barker

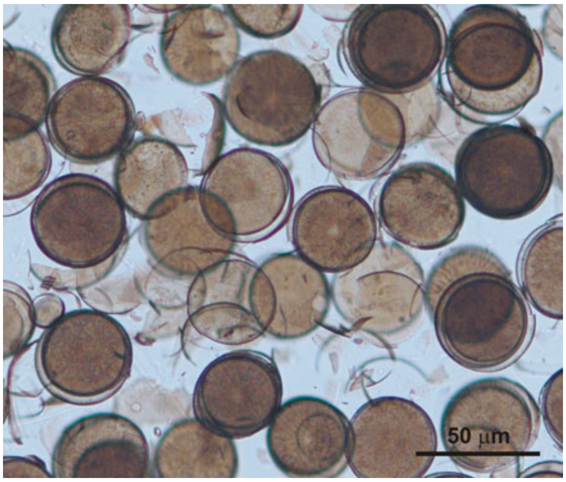

Fig. 4 Diatom-rich sediment from Lago Chungará after the cleaning process. Large *Cyclostephanos andinus* valves are the unique component

2006). Finally, the purified diatom samples were dried at 40°C between 24 h and 48 h. After the cleaning process, all the samples were checked under the light microscope and some of them also with XRD and scanning electron microscope (SEM), as well as analysed for TC to verify that they did not contain any significant amount of terrigenous matter (Fig. 4).

For oxygen isotope analysis, a stepwise fluorination method was applied to 5–10 mg of the purified diatoms in order to strip the frustule hydrous layer before a full reaction with BrF_5 (Leng and Barker 2006). The oxygen liberated was then converted to CO_2 using the method of Clayton and Mayeda (1963), measured by IRMS and normalised against NBS standards. A random selection of 7 samples were analysed in duplicate or triplicate giving a mean reproducibility value of <0.2‰ (1σ), only one sample gave a reproducibility value of 0.4‰ (1σ). The fluorination process and the $^{18}O/^{16}O$ ratios measured were carried out at the NERC Isotope Geosciences Laboratory, British Geological Survey (UK).

We employed two methods of spectral analyses to examine any periodic components in the $\delta^{18}O_{diatom}$ values: Multi-Taper Method (MTM) and Time–Frequency analysis. These two spectral analyses allowed us to examine statistically significant signals in the time series in both the frequency and time domains. MTM provided both a means of spectral estimation and signal reconstruction for time series with spectra that contain both singular and continuous components (Theissen et al. 2008). Time–Frequency (TF) analysis is a hybrid tool between the Fourier Transform and wavelets that intends to use a localised spectrum. For that, this analysis does not use a fixed-size Gaussian window but a Gaussian window that adapts to the spectrum (Stockwell et al. 1996).

All the statistical treatments of the datasets were performed using the R software package (R Development Core Team 2008).

Results

Oxygen isotopes

The $\delta^{18}O_{diatom}$ record (Fig. 5d) shows both short-term (decadal) and long-term oscillations (centennial time scales) ranging from +35‰ to +39.2‰ (mean = +37.4 ± 0.8‰). From the bottom to the top, the studied record can be subdivided into three phases. These intervals correspond to three enrichment/depletion phases (Fig. 5c). Each phase starts with a continuous centennial isotope enrichment which abruptly ends with a sharp depletion:

Phase 1. Lower interval (11,990–11,800 cal year BP). It shows the maximum and minimum $\delta^{18}O_{diatom}$ values (+39.2‰ and +35.1‰ respectively, with a mean value of +37.7 ± 1‰) throughout the whole record. It starts with an increasing trend of ~3.3‰/100 year which finishes at 11,860 cal year BP. This trend is followed by a shift to lighter values of ~8.1‰/100 year with a sharp final decrease in the $\delta^{18}O_{diatom}$ values of 3.5‰ in less than 10 years, acquiring the minimum value for the whole record at ca. 11,800 cal year BP. Both trends are interrupted by ca. 5–20 years depletion/enrichment excursions ranging between ± 0.9 and ± 1.7‰.

Phase 2. Middle interval (11,800–11,550 cal year BP). This section (mean value +37.3 ± 0.7‰) starts with an enrichment trend showing an upwards gradient of ~1.3‰/100 year which finishes at 11,570 cal year BP with a +38.3‰ $\delta^{18}O_{diatom}$ value. This trend is however punctuated by one sudden rise (+2.3‰) and up to four minor depletions (ranging from −0.6 to −1.3‰) of the $\delta^{18}O_{diatom}$ values on a 40–55 years basis. The enrichment trend is followed by a shift of ~9.1‰/100 year to lighter values reaching a minimum value of +36.2‰.

Phase 3. Upper interval (11,550–11,450 cal year BP). This interval (mean value +37.2 ± 0.7‰) also starts with an enrichment trend but, because the section only comprises three samples, this enrichment has not been estimated. This trend is also followed by depletion of 1.3‰ in 10 years.

Spectral analyses of the diatom oxygen isotope record

Multi-taper analysis (MTM) performed on the $\delta^{18}O_{diatom}$ values shows a number of clear periodicities (Fig. 6a). Almost all identified periodicities (7.2, 8.9, 11.1, 13, 18.6, 22.3 and 39.4 years) exceed the 99% confidence interval whereas only two (3.7 and

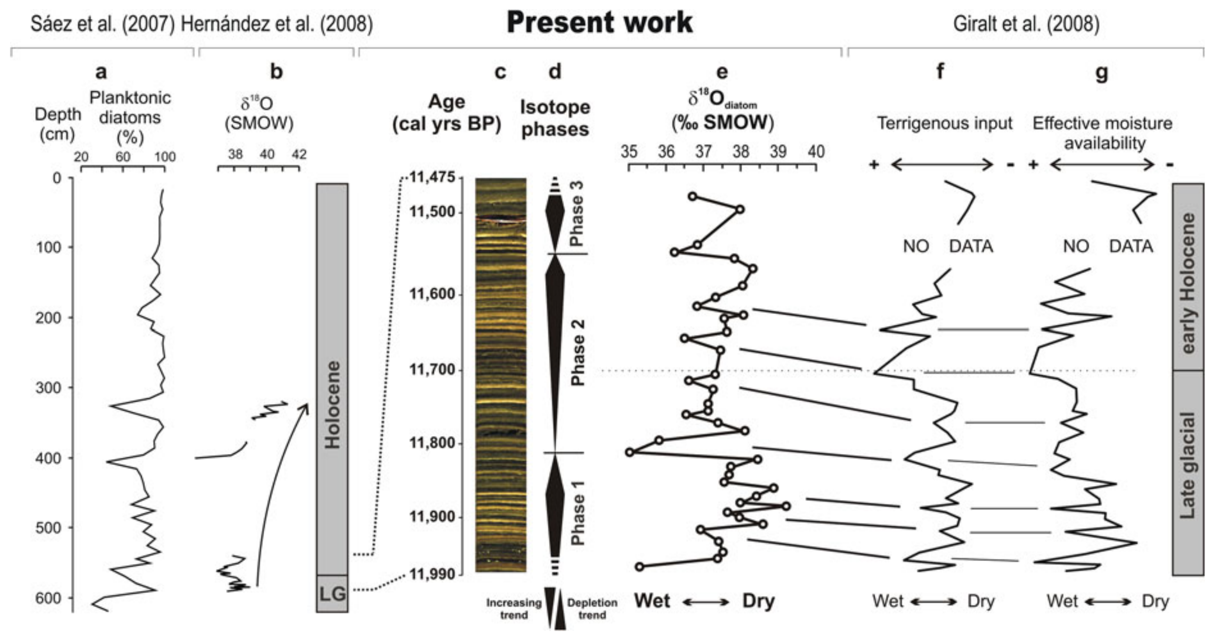

Fig. 5 $\delta^{18}O_{diatom}$ data for the period 11,990–10,475 cal year BP from Lago Chungará, compared with other paleoenvironmental records of the lake. **a** Planktonic diatoms percent abundance curve for the whole Lago Chungará sequence (Sáez et al. 2007). **b** $\delta^{18}O_{diatom}$ data of non-consecutive dark-green laminae from three intervals of the record (Hernández et al. 2008). **c** Photography of laminated sediments corresponding to the sampled interval of subunit 1a in core 11. **d** Oxygen isotope enrichment/depletion phases, in the studied interval, interpreted from the data. **e** $\delta^{18}O_{diatom}$ data from the present study and interpretation in terms of wet and dry conditions. The values correspond to 40 consecutive dark-green laminae throughout the whole selected interval. **f** Terrigenous input variations derived from the first eigenvector of Principal Component Analysis (PCA) on magnetic susceptibility, X-Ray Fluorescence (XRF), X-Ray Diffraction (XRD), Total Carbon and Total Organic Carbon (TC and TOC), Total Biogenic Silica (TBSi) (Giralt et al. 2008). **g** Effective moisture availability variations from the second eigenvector of the mentioned PCA (Giralt et al. 2008). Correlation lines correspond to the main oxygen isotope depletion peaks. Note that the main trends of the three curves are similar but there is a systematic temporal disagreement between them

8 years) lie between 95 and 99% confidence interval (Fig. 6a). Most of the sub-decadal identified frequencies are close to the minimum temporal resolution of the sampling (4.1 years), which explains in great part the weaker intensity of the short periodicities between 3 and 8 years. Therefore, only the most significant frequencies and above the minimum temporal sampling resolution have been taken into account in the discussion.

Time–Frequency (TF) analysis reveals the strongest energy for the lower values of frequency, mainly focussed on the 35-years cycles, whereas it decreases towards higher frequency values, i. e., the higher periodicities (Fig. 6b). This fact can mostly be explained by the decadal sampling resolution, making periodicities lower than 10 years less significant. Additionally, TF analysis indicates that the highest energies of the significant frequencies are located in the late glacial period between ca. 11,950 and 11,700 cal year BP, decreasing just from the onset of the Holocene until, at least, approximately 11,550 cal year BP (Fig. 6b). TF diagram also highlights that the identified frequencies did not have the same intensity (energy) during all the studied period. For instance, the shortest significant periodicity observed in the MTM (7.2 years) was mainly active during the first 150 years of the record, whereas it was only active during three short time windows in the following 500 years. A similar pattern is also observed for the rest of the significant periodicities (8.9, 11.1, 13, 18.6, 22.3 and 39.4 years). The maximum energy areas correspond to depletions in the $\delta^{18}O_{diatom}$ values, i.e. 11,800 and 11,550 cal year BP (Fig. 6b).

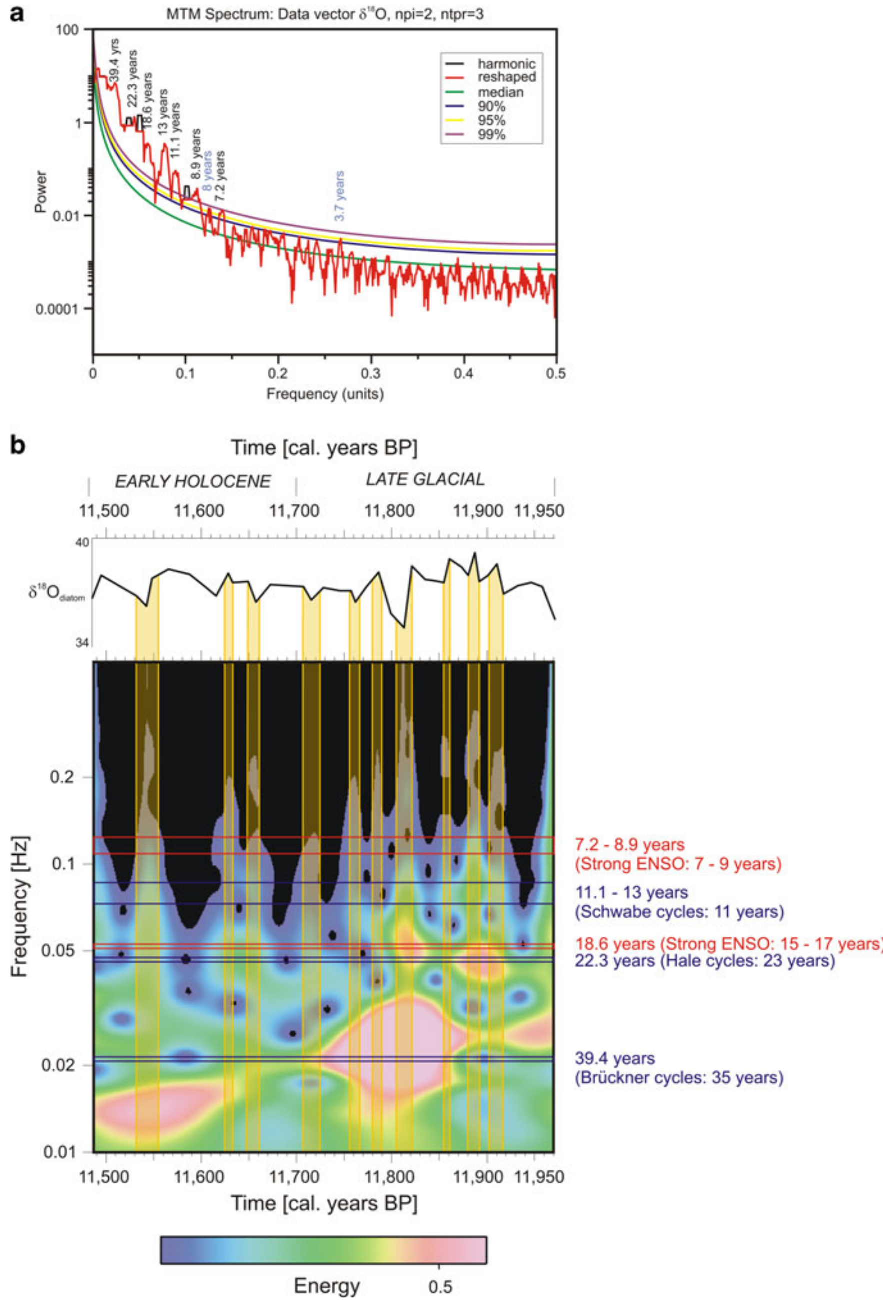

Fig. 6 **a** Multi-taper analysis of the $\delta^{18}O_{diatom}$ values. The 90, 95 and 99% confidence levels are indicated and significant periodicities are shown. Note that periodicities with more than 99% of significance are shown in *black* and those with more than 95% significance in *blue*. **b** Time–Frequency analysis of the $\delta^{18}O_{diatom}$ values. *Pink* indicates high energy whereas *blue* displays low energy areas. Energies below 0.03 were clipped in order to facilitate understanding of the graph. *Red* and *blue horizontal bands* mark different frequency bands of the ENSO and solar activity forcings. *Yellow vertical bands* show zones with $\delta^{18}O_{diatom}$ shifts and their corresponding power values for each frequency. A weakening pattern in ENSO and solar activity energies can be observed through the late glacial-early Holocene transition

Discussion

Controlling factors of $\delta^{18}O_{diatom}$ in Lago Chungará

$\delta^{18}O_{diatom}$ in lake sediments is controlled by the oxygen isotope composition of the lake water ($\delta^{18}O_{lakewater}$), temperature, and the possible disequilibrium by vital effects or diagenesis (Leng and Barker 2006). We discount vital effects and diagenesis as analyses were made on near-monospecific diatom samples and preservation of the diatom frustules is excellent (Fig. 4).

$\delta^{18}O_{lakewater}$ depends on the balance between the isotope composition of water inputs (including the source and amount of precipitation, surface runoff and groundwater inflow) and outputs (evaporation and groundwater loss) in the lake. The measured δ^{18}O of the inputs (springs, Río Chungará and rainfall) in the Lago Chungará is homogeneous, giving values close to the isotope composition of precipitation ($\delta^{18}O_{precipitation}$) (Fig. 3a). $\delta^{18}O_{precipitation}$ is a function of the isotope composition of the moisture source and air-mass trajectory, but in the Lago Chungará there are no changes in the moisture source composition since the air masses always come from the Atlantic Ocean throughout the Amazon basin (Grosjean et al. 1997). During moisture transport from the Atlantic to the lake area, three processes are directly responsible for the low and variable values of the present $\delta^{18}O_{precipitation}$ throughout the Andean Altiplano (Aravena et al. 1999). These processes include interaction of the air masses within the Amazon basin, an altitude effect due to the ascent of the air masses along the eastern slope of the Andes, and the convective nature of the storms in the Altiplano region. Nevertheless, in the Lago Chungará region the values obtained for the measured $\delta^{18}O_{precipitation}$ are relatively stable with almost all values around −14 and −20‰ (Figs. 3a, 3d; Herrera et al. 2006), whereas $\delta^{18}O_{lakewater}$ is much higher (Fig. 3a). This result is in accordance with a $\delta^{18}O_{lakewater}$ enrichment via evaporation. Thus, any isotopic variation of $\delta^{18}O_{lakewater}$ will be more related to changes in the amount of precipitation ("amount effect") and evaporation rather than to the variability of $\delta^{18}O_{precipitation}$. Evaporation enriches δ^{18}O of lake water by 14‰ relative to the inlets (precipitation, springs and river) in the present day (Figs. 3a, 3b; Table 1). During the late glacial and early Holocene the water residence time of the lake was shorter than present because of the different palaeohydrological context, but even so it can be considered closed for that period (Hernández et al. 2008).

Accordingly, the variations in the $\delta^{18}O_{diatom}$ must be mainly derived from changes in the $\delta^{18}O_{lakewater}$ resulted from shifts in the balance between the precipitation and the evaporation (P-E), rather than dominated by temperature. However, two factors should be considered in the interpretation of the $\delta^{18}O_{diatom}$ values in terms of temperature oscillations. The first factor is related to $\delta^{18}O_{precipitation}$ that correlates directly with changes in the air temperature. The global relationship between changes in $\delta^{18}O_{precipitation}$ with air temperature is commonly referred to as the 'Dansgaard relationship', and it implies changes between +0.2 and +0.7‰/°C (Dansgaard 1964). The second is the lakewater temperature dependence of oxygen isotope fractionation between diatom silica and the lake water (Brandriss et al. 1998). Nevertheless, the fractionation factor value of this temperature dependence is still controversial. Published fractionation factors range from −0.2‰ and −0.5‰/°C (Brandriss et al. 1998; Moschen et al. 2005).

The two temperature factors have opposing effects on $\delta^{18}O_{diatom}$ but, owing to its larger variability, the effects of the first factor (air temperature) usually dominate over the second. However, even in the case of the largest change due to the Dansgaard relationship, its magnitude will be greatly damped by the effect of the isotope fractionation between diatom silica and lake water. Moreover, it is known that most of the tropical rainfall isotope datasets exhibit a far stronger correlation with total precipitation than with air temperature (Leng et al. 2005), indicating in the Lago Chungará case a magnification of the P-E balance in wetter periods.

Hence, we can assume that in the Lago Chungará the effects of precipitation variability and temperature oscillations in the $\delta^{18}O_{diatom}$ values will be small in comparison to evaporative concentration, as pointed by other authors for closed lakes in general (Gat 1980; Gasse and Fontes 1992).

Variations of the precipitation-evaporation balance in the lake

Oxygen isotopes have widely been used to carry out lake level reconstructions and to establish consequent palaeoclimatic interpretations (Barker et al. 2001; Valero-Garcés et al. 2003).

There is a relationship between lake level change and the P-E balance for Lago Chungará during the late glacial and early Holocene, but this dependency is hampered by local palaeohydrological factors such as changes in the groundwater outflow and shifts in the lake surface/volume ratio which produce a background long term enrichment trend (Hernández et al. 2008). This effect is however negligible when considering isotopic changes at a decadal to centennial time scale. Both present (Fig. 3) and past (Thompson et al. 1998) rainfall isotope values in the Lago Chungará region are much lighter than those measured for the lakewater, and the magnitude of the long-term enrichment trend is very small compared to them. Therefore, depletions of $\delta^{18}O_{diatom}$ would directly be related to wet episodes in the Andean Altiplano, whereas exceptionally high values, which stand out over the general enrichment trend, would indicate arid episodes.

The observed $\delta^{18}O_{diatom}$ enrichment trends agree with periods where light-white laminae are more common, whereas depletion episodes coincide with poorly developed and less abundant light-white laminae (Figs. 5c, 5d). These light-white laminae are most likely the result of exceptional periods of mixing of the shallow water column during low-stands, which recycle nutrients from the hypolimnion and therefore trigger extraordinary diatom blooms (Hernández et al. 2007). This interpretation is also supported by terrigenous input and regional effective moisture reconstructions previously performed on the Lago Chungará sedimentary record (Giralt et al. 2008) (Figs. 5f, 5g). These reconstructions were carried out by applying multivariate statistical analyses (Cluster, Redundancy Analysis (RDA) and Principal Component Analysis (PCA)) to magnetic susceptibility, XRF, XRD, TC, TOC, TBSi and grey-colour curve data. The terrigenous inputs curve was derived from the first eigenvector of the PCA, whereas the regional effective moisture reconstruction was obtained from the second eigenvector. For the lower part of Chungara sequence (Unit 1), the more positive values of the terrigenous inputs were interpreted, as increasing erosion rate of catchment volcanic sediments, suggesting humid conditions. Similarly, the effective moisture availability proxy depends on the P-E balance, with positive values corresponding to drier conditions (Giralt et al. 2008). The comparison of the three proxies (Figs. 5e, 5f, 5g) shows that the hydrological response of the diatom silica oxygen isotopes (a biological proxy) and of the other two reconstructions to the environmental variations is not the same.

The main trends in the three curves (Figs. 5e, 5f, 5g) are similar but there is a systematic temporal disagreement (ranging between ca. 5 and 50 cal year BP) between the terrigenous inputs and the regional effective moisture availability (which both react first) and the $\delta^{18}O_{diatom}$ (reacting afterwards). This time lag between the two proxies highlights the complex and non-linear response of the lacustrine ecosystem to environmental forcings (Fritz 2008). After rainfall the increased runoff and input of terrigenous material is almost immediate. On the contrary, the oxygen isotope homogenisation of the lakewater which later will be incorporated on the diatom frustule, has a delayed time of response. This depends on the epilimnion water residence time and, furthermore, whether the lake is hydrologically closed or not. Hence, the observed time lag can be showing these different responses of the system to the same forcing. However, we cannot discount the poorly understood concept of silica maturation, where pores in the silica matrix close through early diagenesis creating differences in the $\delta^{18}O$ between living diatoms and sediment assemblages (Schmidt 2001) and therefore a lag in the $\delta^{18}O_{diatom}$ record.

At centennial scale, the Lago Chungará isotopic values show a general pattern of increasing $\delta^{18}O_{diatom}$ (Fig. 5b), with an enhanced enrichment period at the bottom, but interrupted by three major depletion events. The depletion events, accentuated by the "amount effect", correspond to heavy rainfall conditions, whereas enriched values would indicate exceptionally dry conditions favouring the evaporation. This interpretation is reinforced by the terrigenous input and effective regional moisture availability independent reconstructions.

Three wet/dry phases have been identified in the $\delta^{18}O_{diatom}$ record (Fig. 5d). Phase 1 (11,990–11,800 cal year BP) shows a significantly increased gradient in $\delta^{18}O_{diatom}$ suggesting that dominantly dry climate conditions played a key role triggering this isotope enrichment. Because of this drier situation the lake level would be lower, as also indicated by the important development and major presence of light-white laminae in this part of the interval. Three low-intensity and short-term wet episodes punctuate the established late glacial arid period (Fig. 5e). These episodes can also be recognised and correlated with events of increased terrigenous inputs and effective moisture availability (Figs. 5e, 5f, 5g).

The much weaker isotope enrichment for phase 2 (11,800 and 11,550 cal year BP) can be mainly ascribed to the general low magnitude palaeohydrological background trend towards heavier isotope conditions of the late glacial-early Holocene transition (Hernández et al. 2008). This fact, together with the poorer development and minor presence of the light-white laminae with respect to the previous interval, suggests that the enrichment via evaporation was much less important than during the sedimentation of phase 1, corresponding to a more humid period. Furthermore, the terrigenous inputs and effective regional moisture availability curves show relatively wetter conditions for this period (Figs. 5f, 5g). This trend is also punctuated by a sudden rise in the lowest part of the interval indicating a short dry event and slight depletions in $\delta^{18}O_{diatom}$ indicating wet decadal-scale events (Fig. 5e).

In phase 3 any clear trend is difficult to identify (Fig. 5e). Although the $\delta^{18}O_{diatom}$ record seems to show a new trend towards drier conditions after the sudden wet event dated at 11,550 cal year BP, the lack of suitable samples has hampered any firm conclusions.

Long-term, centennial- to millennial-scale palaeoclimatic implications

There are many Late Quaternary palaeoclimatic reconstructions from the Andean Altiplano region (Sylvestre et al. 1999; Rigsby et al. 2005) but the climatic context for the late glacial-Holocene transition still remains unclear. Some authors have defined a cold period (12,600–11,500 cal year BP) coincident with the Northern hemisphere's Younger Dryas event (Baker et al. 2001b). The wet ("Coipasa phase", Thompson et al. 1998; Placzek et al. 2006) or dry (Maslin and Burns 2000; Weng et al. 2006) character of this event remains controversial. On the contrary, other authors consider this period just the final part of the deglaciation towards the present interglacial ("Ticaña phase", Sylvestre et al. 1999), as part of a long-term dry pattern (Rowe et al. 2002; Abbott et al. 2003).

The previous lake level reconstruction, mainly based on the abundance of planktonic diatoms, shows a shallowing followed by a long term rising trend for the interval presented here (Sáez et al. 2007). Additionally, recent data on the Lago Chungará record, mainly based on XRF core scanner analysis, has established the late glacial to Holocene transition as a relatively wet period (Giralt et al. 2008). The centennial scale $\delta^{18}O_{diatom}$ record is congruent with the lake level reconstruction performed by Sáez et al. (2007) which represents the palaeoclimatic evolution related to the major lake level variations (Fig. 5a). The non-continuous isotopic data (Fig. 5b) also displays a persistent, but minor, background isotope enrichment trend. This enrichment is related to changes in the lake morphology due to shifts in its surface/volume ratio, as well as changes in the groundwater outflow during the lake ontogeny (Hernández et al. 2008). In any case, the new $\delta^{18}O_{diatom}$ data presented here highlights that the glacial-interglacial transition in the central Andean Altiplano was punctuated by abrupt and high-frequency centennial climatic variability.

Short-term, decadal- to centennial-scale palaeoclimatic implications

Millennial-scale shifts in the Atlantic-Amazon-Altiplano hydrologic system have been attributed to orbitally induced changes in solar insolation, coupled with long-term changes in the ENSO variability (Rowe et al. 2002; Abbott et al. 2003; Servant and Servant-Vildary 2003). However, higher-resolution changes are not directly related to orbitally induced insolation forcing (Abbott et al. 2003). The interannual climate variability in the Andean Altiplano is most likely related to changes in the Pacific Tropical SSTs, and the sign and strength of the zonal winds above the Altiplano (Garreaud et al. 2003). Both factors would affect the strength and position of the Bolivian high and, hence, the moisture distribution over the region. The main force controlling the SSTs is the ENSO variability, involving dry or wet situations in the Altiplano during El Niño- or La Niña-like conditions respectively (Garreaud et al. 2003; Vuille and Werner 2005). This is consistent with instrumental data from the Chungará area where precipitation is reduced during moderate to intense El Niño years (1965, 1972, 1983, and 1992) (Fig. 3c). Additionally, the sign and strength of the zonal winds above the Altiplano would be modulated by decadal and multidecadal variations in solar activity, possibly related to the mode of the ENSO system (Theissen et al. 2008). Although ENSO modulation by solar activity has been suggested (Velasco and Mendoza 2008), no clear relationship has been demonstrated between both forcings. Nevertheless, there is broad agreement that ENSO events are the main control governing the moisture distribution in the Altiplano (Servant and Servant-Vildary 2003), and that decadal-scale changes in the effective moisture could be related to the solar activity during the mid-Holocene (Theissen et al. 2008).

The results presented here would suggest a similar pattern during the late glacial-Holocene transition over the Andean Altiplano (Fig. 6b). The identified frequencies can be attributed to different periodicities of the solar activity cycles such as Schwabe 11 years (identified as 11.1 and 13 years), Hale 23 years (22.3 years) and Brückner 35 years (39.4 years), and of the ENSO frequency (main frequency at 7–9 years (7.2 and 8.9 years) and its decadal frequency 15–17 years (18.6 years)). The influence of solar activity and ENSO variability on the isotope record is supported by the fact that several periodicities concordant with both forces were identified. The time–frequency analysis suggests that the driest period (11,950–11,800 cal year BP) was ruled by high solar activity, mainly represented by a Brückner cycle, and strong ENSO-like conditions.

The ENSO and solar activity signals remain present for the early Holocene period (between 11,750 until 11,500 cal year BP), although they show a weakening pattern through this period (Fig. 5b). This fact is congruent with the progressive weakening of the ENSO suggested by other authors for the late glacial-Holocene transition (Rodbell et al. 1999; Moy et al. 2002; Rodó and Rodríguez-Arias 2004). In Lago Chungará, the onset of the Holocene was characterised by minor $\delta^{18}O_{diatom}$ enrichment by evaporation and by the occurrence of multi-decadal weak depletions that would be governed by the more humid La Niña-like conditions. This would agree with previous observations that suggest a reduction in the El Niño intensity within the region during the early-Holocene in favour of long-term La Niña-like conditions in the tropical Pacific (Betancourt et al. 2000; Koutavas et al. 2002).

Conclusions

The late glacial to Holocene transition from the Lago Chungará record is made up of laminated diatom-rich sediments which provide excellent material for the application of oxygen isotope analysis in biogenic silica. $\delta^{18}O_{diatom}$ data have for the first time provided palaeoclimatic reconstruction at decadal-to-centennial resolution. The well-laminated nature of these sediments allowed a lamina by lamina continuous sampling, giving one of the highest resolution records available for $\delta^{18}O_{diatom}$. It has also revealed important insights into the usefulness of this method, as well as provided decisive palaeoenvironmental information for this critical period.

$\delta^{18}O_{diatom}$ from dark-green diatom laminae represent the baseline in the environmental evolution of Lago Chungará, and show decadal to centennial variability in the moisture conditions of the Andean Altiplano. The isotopic record displays a persistent background isotope enrichment trend related to changes in the lake morphology and groundwater outflow during the late glacial and early Holocene. Overprinted onto this long-term (centennial to millennial) trend there are cyclically short-term (decadal to centennial) shifts which are not related to changes in temperature or isotopic composition of the source of precipitation, but to the P-E balance variability in the Altiplano.

The record shows two major isotope depletions, occurring at a centennial time scale (11,800 and 11,550 cal year BP) indicating a long-term increase in moisture conditions, and one major isotope enrichment above the background levels that occurred between 11,990 and 11,800 cal year BP indicating a short dry phase during the late glacial. Minor depletions at a decadal time scale are associated with weaker rainfall short-term events. The comparison with terrigenous input and effective moisture availability reconstructions previously performed for Lago Chungará shows agreement, but includes a systematic time lag (up to 50 years) among these proxies and $\delta^{18}O_{diatom}$. This is mainly due to the time necessary to change the $\delta^{18}O_{lakewater}$ values and its subsequent incorporation into the diatom frustules, but other factors should not be completely disregarded. The time lag highlights the fact that not all the proxies react at the same time to environmental forcing and this needs to be more often recognised in high resolution palaeolimnological reconstructions.

Sub-millennial shifts in the hydrological balance of Lago Chungará are hypothesised to be the result of changes in the strength and position of the Bolivian High. Spectral analyses of $\delta^{18}O_{diatom}$ suggest that these changes in the atmospheric conditions over the Altiplano during the wet events were triggered by both ENSO and solar activity. The change from the late glacial dry period to a wetter early Holocene period confirms a weakening of El Niño intensity in the Andean Altiplano region in favour of La Niña-like conditions found elsewhere. Nested upon the underlying climate dynamics are the different cyclicities of solar activity (Schwabe, Hale and Brückner) that were active during different time windows. There is undoubtedly an interaction between these and ENSO at the decadal and greater scales and it is likely that apparent solar forcing of the Lago Chungará record is transmitted via ENSO modulation of the South American monsoon. The complexity of Andean Altiplano palaeoenvironmental conditions, and the absence of other high resolution studies for this time interval, does not allow us to establish any clear conclusion on the existence of significant climatic events synchronous to the Younger Dryas in the northern hemisphere. While many studies have demonstrated ENSO-like forcing during the glacial-interglacial transition, this highly resolved record is one of the few that preserves key ENSO frequencies, therefore further implicating this major climatic process with events governing the transition to the Holocene.

Acknowledgments The Spanish Ministry of Science and Innovation funded the research at Lago Chungará through the projects ANDESTER (BTE2001-3225), Complementary Action (BTE2001-5257-E), LAVOLTER (CGL2004-00683/BTE), GEOBILA (CGL2007-60932/BTE) and CONSOLIDER-Ingenio 2010 GRACCIE (CSD2007-00067). A. Hernández have benefited from a FPI grant from The Spanish Ministry of Science and Innovation. The Limological Research Center (USA) provided the technology and expertise to retrieve the cores. We are grateful to CONAF (Chile) for the facilities provided in Chungará. The NIGL (UK) funded the isotope analysis, and Hilary Sloane is specially thanked for assistance with the diatom oxygen isotope measurements.

References

Abbott MB, Wolfe BB, Wolfe AP, Seltzer GO, Aravena R, Mark BG, Polissar PJ, Rodwell DT, Rowe HD, Vuille M (2003) Holocene paleohydrology and glacial history of the central Andes using multiproxy lake sediment studies. Palaeogeogr Palaeoclimatol Palaeoecol 194:123–138. doi:10.1016/s0031-0182(03)00274-8

Aravena R, Suzuki O, Peña H, Pollastri A, Fuenzalida H, Grilli A (1999) Isotopic composition and origin of the precipitation in northern Chile. Appl Geochem 14:411–422

Baker PA, Seltzer GO, Fritz SC, Dunbar RB, Grove MJ, Tapia PM, Cross SL, Rowe HD, Broda JP (2001a) The history of South American tropical precipitation for the past 25, 000 years. Science 291:640–643

Baker PA, Rigsby CA, Seltzer GO, Fritz SC, Lowenstein TK, Bacher NP, Veliz C (2001b) Tropical climate changes at millennial and orbital timescales on the Bolivian Altiplano. Nature 409:698–701

Barker PA, Street-Perrott FA, Leng MJ, Greenwood PB, Swain DL, Perrott RA, Telford RJ, Ficken KJ (2001) A 14 ka oxygen isotope record from diatom silica in two alpine tarns on Mt Kenya. Science 292:2307–2310

Barker PA, Leng MJ, Gasse F, Huang Y (2007) Century-to-millennial scale climatic variability in Lake Malawi revealed by isotope records. Earth Planet Sci Lett 261:93–103. doi:10.1016/j.epsl.2007.06.010

Betancourt JL, Latorre C, Rech JA, Quade J, Rylander KA (2000) A 22,000-year record of monsoonal precipitation from Northern Chile's Atacama Desert. Science 289: 1542–1546

Brandriss ME, O'Neil JR, Edlund MB, Stoermer EF (1998) Oxygen isotope fractionation between diatomaceous silica and water. Geochim Cosmochimi Acta 62:1119–1125

Brewer TS, Leng MJ, Mackay AW, Lamb AL, Tyler JJ, Marsh NG (2008) Unravelling contamination signals in biogenic silica oxygen isotope composition: the role of major and trace element geochemistry. J Quat Sci 23:321–330. doi: 10.1002/jqs.1171

Clayton RN, Mayeda TK (1963) The use of bromine pentafluoride in the extraction of oxygen from oxide and silicates for isotope analysis. Geochim Cosmochim Acta 27:43–52

Dansgaard W (1964) Stable isotopes in precipitation. Tellus 16:436–468

Dorador C, Pardo R, Vila I (2003) Variaciones temporales de parámetros físicos, químicos y biológicos de un lago de altura: el caso del Lago Chungará. Rev Chil Hist Nat 76:15–22

Fritz SC (2008) Deciphering climatic history from lake sediments. J Paleolimnol 39:5–16. doi:10.1007/s10933-007-9134-x

Garreaud RD, Vuille M, Clement AC (2003) The climate of the Altiplano: observed current conditions and mechanisms of past changes. Palaeogeogr Palaeoclimatol Palaeoecol 194:5–22. doi:10.1016/S0031-0182(03)00269-4

Gasse F, Fontes JC (1992) Climatic changes in northwest Africa during the last deglaciation (16–7 ka BP). NATO ASI Series 12. Kluwer, Dordrecht, pp 295–325

Gat JR (1980) Isotope hydrology of very saline lakes. In: Nissenbaum A (ed) Hypersaline brines and evaporitic environments. Elsevier, Amsterdam, pp 1–8

Giralt S, Moreno A, Bao R, Sáez A, Prego R, Valero BL, Pueyo JJ, González-Sampériz P, Taberner C (2008) Statistical approach to distangle environmental forcings in a lacustrine record: the Lago Chungará case (Chilean Altiplano). J Palaeolimnol 40:195–215. doi:10.1007/s10933-007-9151-9

Grosjean M, Valero-Garcés B, Geyh MA, Messerli B, Schreier H, Kelts K (1997) Mid and late holocene limnogeology of laguna del negro francisco, northern chile, and its paleoclimatic implications. The Holocene 7:151–159

Grosjean M, van Leeuwen JFN, van der Knaap WO, Geyh MA, Ammann B, Tanner W, Messerli B, Núñez L, Valero-Garcés BL, Veit H (2001) A 22,000 14C year BP sediment and pollen record of climate change from Laguna Miscanti (23°S), Northern Chile. Glob Planet Change 28:35–51

Hernández A, Bao R, Giralt S, Leng MJ, Barker PA, Pueyo JJ, Sáez A, Moreno A, Valero-Garcés B, Sloane HJ (2007) A high-resolution study of diatom oxygen isotopes in a Late Pleistocene to Early Holocene laminated record from Lake Chungará (Andean Altiplano, Northern Chile). Geochim Cosmochim Acta 71:A398

Hernández A, Bao R, Giralt S, Leng MJ, Barker PA, Sáez A, Pueyo JJ, Moreno A, Valero-Garcés BL, Sloane HJ (2008) The palaeohydrological evolution of Lago Chungará (Andean Altiplano, northern Chile) during the Lateglacial and early Holocene using oxygen isotopes in diatom silica. J Quat Sci 23:351–363. doi:10.1002/jqs.1173

Herrera C, Pueyo JJ, Sáez A, Valero-Garcés BL (2006) Relación de aguas superficiales y subterráneas en el área del lago Chungará y lagunas de Cotacotani, norte de Chile: un estudio isotópico. Rev Geol Chile 33:299–325

Hora J, Singer B, Wörner G (2007) Volcano eruption and evaporative flux on the thick curst of the Andean Central Volcanic Zone: $40^{Ar}/39^{Ar}$ constrains from Volcán Parinacota, Chile. Geol Surv Am Bull 119:343–362. doi:10.1130/B25954.1

Juillet-Leclerc A (1986) Cleaning process for diatomaceous samples. In: Ricard M (ed) 8th diatom symposium. Koeltz Scientific Books, Koenigstein, pp 733–736

Koutavas A, Lynch-Stieglitz J, Marchitto T, Sachs J (2002) El Niño-like pattern in ice age tropical Pacific sea surface temperature. Science 297:226–230

Leng MJ, Barker PA (2006) A review of the oxygen isotope composition of lacustrine diatom silica for palaeoclimate reconstruction. Earth Sci Rev 75:5–27. doi:10.1016/j.earscirev.2005.10.001

Leng MJ, Lamb AL, Heaton THE, Marshall JD, Wolfe BB, Jones MD, Holmes JA, Arrowsmith C (2005) Isotopes in lake sediments. In: Leng MJ (ed) Isotopes in palaeoenvironmental research. Springer, Dordrecht, pp 147–184

Maslin MA, Burns SJ (2000) Reconstruction of the Amazon Basin effective moisture availability over the past 14,000 years. Science 290:2285–2287

Moreno A, Giralt S, Valero-Garcés BL, Sáez A, Bao R, Prego R, Pueyo JJ, González-Sampériz P, Taberner C (2007) A 13 kyr high-resolution record from the tropical Andes: The Chungará Lake sequence (18°S, northern Chilean Altiplano). Quat Int 161:4–21. doi:10.1016/j.quaint.2006.10.020

Morley DW, Leng MJ, Mackay AW, Sloane HJ, Rioual P, Battarbee RW (2004) Cleaning of lake sediment samples for diatom oxygen isotope analysis. J Paleolimnol 31:391–401

Moschen R, Lücke A, Schleser G (2005) Sensitivity of biogenic silica oxygen isotopes to changes in surface water temperature and palaeoclimatology. Geophys Res Lett 32:L07708. doi:10.1029/2004GL022167

Moy CM, Seltzer GO, Rodbell DT, Anderson DM (2002) Variability of El Niño/Southern Oscillation activity at millenial timescales during the Holocene epoch. Nature 420:162–165

Mühlhauser H, Hrepic N, Mladinic P, Montecino V, Cabrera S (1995) Water-quality and limnological features of a high-altitude andean lake, Chungará in northern chile. Rev Chil Hist Nat 68:341–349

Negri AJ, Adler RF, Shepherd JM, Huffman G, Manyin M, Neklin EJ (2004) A 16-year climatology of global rainfall from SSM/I highlighting morning versus evening differences. 13th Conference on Satellite Meteorology and Oceanography. American Meteorological Society, Norfolk, VA P6. 16

Placzek C, Quade J, Patchett PJ (2006) Geochronology and stratigraphy of late Pleistocene lake cycles on the southern Bolivian Altiplano: Implications for causes of tropical climate change. Geol Soc Am Bull 118:515–532. doi:10.1130/B25770.1

Rietti-Shati M, Shemesh A, Karlen W (1998) A 3000-year climatic record from biogenic silica oxygen isotopes in an equatorial high-altitude lake. Science 281:980–982

Rigsby CA, Bradbury JP, Baker PA, Rollins SM, Warren MR (2005) Late Quaternary palaeolakes, rivers, and wetlands on the Bolivian Altiplano and their palaeoclimatic implications. J Quat Sci 20:671–691. doi:10.1002/jqs.986

Rings A, Lucke A, Schleser GH (2004) A new method for the quantitative separation of diatom frustules from lake sediments. Limnol Oceanogr Methods 2:25–34

Rodbell DT, Seltzer GO, Anderson DM, Abbott MB, Enfield DB, Newman JH (1999) An 15, 000-year record of El Niño-driven alluviation in southwestern Ecuador. Science 283:516–520

Rodó X, Rodríguez-Arias MA (2004) El Niño–Southern oscillation: absent in the early holocene? J Clim 17:423–426

Rowe HD, Dunbar RB, Mucciarone DA, Seltzer GO, Baker PA, Fritz S (2002) Insolation, moisture balance and climate change on the South American Altiplano since the Last Glacial Maximum. Clim Change 52:175–199

Sáez A, Valero-Garcés BL, Moreno A, Bao R, Pueyo JJ, González-Sampériz P, Giralt S, Taberner C, Herrera C, Gibert RO (2007) Volcanic controls on lacustrine sedimentation: The late Quaternary depositional evolution of lake Chungará (Northern Chile). Sedimentology 54:1191–1222. doi:10.1111/j.1365-3091.2007.00878.x

Servant M, Servant-Vildary S (2003) Holocene precipitation and atmospheric changes inferred from river paleowetlands in the Bolivian Andes. Palaeogeogr Palaeoclimatol Palaeoecol 194:187–206

Stockwell RG, Mansinha L, Lowe RP (1996) Localization of the complex spectrum: the S transform. IEEE TSP 44:998–1001

Sylvestre F, Servant M, Servant-Vildary S, Causse C, Fournier M, Ybert J-P (1999) Lake-level chronology on the southern Bolivian Altiplano (18°–23°S) during late-glacial time and the early Holocene. Quat Res 51:54–66

R Development Core Team (2008) R: a language and environment for statistical computing. R Foundation for statistical computing, Vienna, Austria ISBN 3-900051-07-0. http://www.R-project.org

Theissen KM, Dunbar RB, Rowe HD, Mucciarone DA (2008) Multidecadal- to century-scale arid episodes on the Northern Altiplano during the middle Holocene. Palaeogeogr Palaeoclimatol Palaeoecol 257:361–376. doi:10.1016/j.palaeo.2007.09.011

Thompson LG, Davis ME, Mosley-Thompson E, Sowers TA, Henderson KA, Zagorodnov VS, Lin PN, Mikhalenko VN, Campen RK, Bolzan JF, Cole-Dai J, Francou B

(1998) A 25, 000-year tropical climate history from Bolivian ice cores. Science 282:1858–1864

Valero-Garcés BL, Grosjean M, Schwalb A, Schreir H, Kelts K, Messerli B (2000) Late Quaternary lacustrine deposition in the Chilean Altiplano (18°–28°S). In: Gierlowski-Kordech E, Kelts K (eds) Lake basins through space and time. Studies in Geology 46. Am Assoc Petr Geol, pp 625–636

Valero-Garcés BL, Delgado-Huertas A, Navas A, Edwards L, Schwalb A, Ratto N (2003) Patterns of regional hydrological variability in central-southern Altiplano (18°-26°S) lakes during the last 500 years. Palaeogeogr Palaeoclimatol Palaeoecol 194:319–338

Velasco VM, Mendoza B (2008) Assessing the relationship between solar activity and some large scale climatic phenomena. Adv Space Res 42:866–878. doi:10.1016/j.asr.2007.05.050

Vuille M, Werner M (2005) Stable isotopes in precipitation recording South American summer monsoon and ENSO variability: observations and model results. Clim Dyn 25:401–413. doi:10.1007/s00382-005-0049-9

Weng C, Bush MB, Curtis JH, Kolata AL, Dillehay TD, Binford MW (2006) Deglaciation and Holocene climate change in the western Peruvian Andes. Quat Res 66:87–96. doi:10.1016/j.yqres.2006.01.004